International Journal of Food Engineering

Volume 1, *Issue* 1 2005 *Article* 5

Thermal Sterilisation of Liquid Foods in a Sealed Container – Developing Simple Correlations to Account for Natural Convection

Xiao Dong Chen* Hua-Jiang Huang†

Abdul G. Ghani‡

*Food and Bioproduct Processing Cluster, Department of Chemical and Materials Engineering, University of Auckland, New Zealand; Corresponding author , dong.chen@eng.monash.edu.au

†UNILAB Research Centre of Chemical Reaction Engineering, East China University of Science and Technology, Shanghai, PR China , huanghuajiang@hotmail.com

‡Food and Bioproduct Processing Cluster, Department of Chemical and Materials Engineering, University of Auckland, New Zealand, a.ghani@auckland.ac.nz

Thermal Sterilisation of Liquid Foods in a Sealed Container – Developing Simple Correlations to Account for Natural Convection

Xiao Dong Chen, Hua-Jiang Huang, and Abdul G. Ghani

Abstract

In this study, two approaches to developing simple correlations have been described and analysed. The recent 'effective thermal diffusivity' model has been benchmarked and the advantages of the approach illustrated. The 'uniqueness' of this kind of approach has been discussed. The second approach, which is new and called the 'effective velocity' approach, has been described and tested, against the limited data sets available. It has been demonstrated that by preserving the first order effect (i.e. the convection effect) in the heating equation, the second approach gives an opportunity to correlate with good accuracy the experimental data (whether it is generated by CFD or field measurement). Here the essential features of the natural convection driven process is captured well. The predicted circulation velocity level matches well with the previous CFD simulations for the two dimensional situations, supporting the validity of the approach. More in depth and quantitative study is required before any of these models can be used in practice.

KEYWORDS: thermal processing, natural convection, thermal diffusivity, modelling

1. INTRODUCTION

Thermal processing is referred to the processes that heat, hold and cool a food product sequentially, which is required to be free of food-borne illness for a desired period of time. Pasteurization is a type of thermal processing, which reduces the potential of contamination of a special pathogenic micro-organism to a desired extent, fulfilling the shelf-life requirement. The product will, in many cases, still need to be refrigerated otherwise it will not be shelf-stable. Sterilization is the process that leads to shelf-stable products in cans, soft containers or bottles (Singh and Heldman, 1993). This process usually employs much greater temperature than pasteurization.

Because of the geometrical complexity and also the involvement of natural convection of liquid inside various types of containers for sterilisation, detailed simulation studies have been performed using commercially available Computational Fluid Dynamics (CFD) software. The simulations have been carried out to investigate the interactions of the fluid movement, heat transfer and species (bacteria, vitamins etc) transfer.

The existence and where-about of the so-called 'slowest heating zone (SHZ) or the coldest zone', where the temperature of the fluid is the lowest, and its reduction over sterilization time is the primary subject of practical interest. Due to the fluid movement, stagnation zone (usually within a recirculation zone) is also of a primary interest as the microbes or nutrient species would not be transported that easily out of stagnant zone. Therefore, the movement and evolution of the SHZ, is an important aspect for CFD analysis to explore, e.g. the work by Datta and Teixeira (1987, 1988) and that by Kumar et al (1990). Without the presence of natural convection, only conduction is considered, one will find the slowest heating zone can only be located at the geometrical centre, which is in most cases unrealistic for liquid containing products.

If the filled material in a can or a pouch is basically solid, there would be no fluid movement. In this case, heat conduction and species diffusion within the solid matrix can be readily resolved according to classical theories and using relatively simple numerical procedures. Previous studies which used conduction mode as the only heat transfer mechanism pointed to the CZ being the geometrical centre. For a vertically placed cylindrical can in a retort device, CZ or the coldest point (CP) is located right at the centre of the central axis.

When the fluid flow is involved, CFD is usually required, under two or three-dimensional situations. The process of can sterilization must involve CFD in order to locate the SHZ. Though CFD is powerful in the ease of providing the details of the flow, temperature and concentration fields, the interpretation of the simulation results and laboratory validations are all very important aspects of the CFD modeling exercises. CFD packages required experienced, usually researchers who have spent reasonable amount of time on using the packages. Usually for each case it computes, CFD takes some hours to finish. As a practical, simple and swift prediction tool, CFD is not yet the most sensible method. In any case, for either can sterilization or pouch sterilization processes, one can look up the recent series of important CFD and experimental studies carried out by Ghani (2002) and Ghani et al (1999-2002). These studies have established the details of fluid flow, temperature distribution and concentration distribution inside the sealed containers. Though CFD is available for food engineering researchers to explore the details of thermal processing, it is not a suitable means for practising engineers. There is a need for developing simple models which can be easily implemented using Excel spreadsheet and the like.

Having discovered the details of the fluid motion and the evolution of the slowest heating zone, it is desirable to obtain a semi-empirical formula, which encapsulates the major aspects of the mechanisms involved but at the same time provides a fast and economical means of computation compared with CFD analysis. To this end, a recent study by Farid and Ghani (2004) was an attempt to achieve this objective, by considering an established concept of effective thermal diffusivity to account for natural convection. A close examination of such an approach from a fundamental view point is provided as a benchmark study. The section after the following one will be dedicated to a fundamental procedure, which has been developed to allow natural convection effect to be accounted for with a convection term (a first order effect) in the one-dimensional energy balance.

2. ON EFFECTIVE THERMAL DIFFUSIVITY APPROACH

Most recently, a simple calculation procedure for calculating the temperature of the SHZ has been proposed by Farid and Ghani (2004). They considered the sterilisation of the sealed containers (vertical or horizontal cans) and a generalised correlation had been developed. The essence of the approach is to consider the process as an 'effective' conduction type process, but incorporating an effective thermal conductivity (k_e) (Holman, 1976):

$$k_e = k \cdot Nu_\delta \tag{1}$$

where k is the original conductivity (W.m^{-1}.K^{-1}) and Nu_δ is the Nusselt number based on the characteristic dimension δ (m) (for vertically placed can, this is taken to be the radius of the can). Equation (1) accounts for the effect of convection. The Nusselt number relationship used was similar to that of natural convection in a two-dimensional enclosed vertical space with one wall is hot and another is cold whilst the top and bottom surfaces are adiabatic (the enclosure's height is at least twice as much as the width (δ) but smaller than 10 times of the width):

$$\overline{Nu}_L = 0.22\left(\frac{\mathrm{Pr}}{0.2+\mathrm{Pr}}Ra_L\right)^{0.28}\left(\frac{H}{\delta}\right)^{-0.25} \tag{2}$$

where the height (H, m) was taken to be the height of the can. All properties are calculated at film temperature except for the density and specific heat capacity of the CMC solutions and Carrot-orange soup. The driving force in Rayleigh number calculations was the temperature difference ($T_\infty - T_{SHZ}$). T_∞ is the sterilisation temperature (steam condensing temperature) which is usually 121 °C. T_{SHZ} is the temperature of the slowest heating zone (SHZ) or say the smallest temperature in a can of fluid being thermally processed. The exponent of H/δ term (which is -0.25 in equation (2)) was left to be an adjustable parameter. The viscosities were taken to be temperature dependent. The thermal expansion coefficients for CMC solutions and Carrot-orange soup were taken to be constant (0.0002 K^{-1}). The dimensionless temperature was then defined as the following:

$$\theta^* = \frac{T_\infty - T_{SHZ}}{T_\infty - T_o} \tag{3}$$

DOI: 10.2202/1556-3758.1006

where T_o is the initial (uniform) temperature (°C) and T_∞ is the final temperature which is equal to the steam condensing temperature of 121 °C at the can surfaces. The temperature of the slowest heating zone (the lowest temperature in the can), T_{SHZ}, is a function of location and time.
With the Fourier number defined as follows:

$$F_o = \frac{\alpha_e \cdot t}{\left(2 \cdot \frac{V}{A}\right)^2} \qquad (4)$$

where, α_e is the effective thermal diffusivity ($=k_e/\rho c_p$) ($m^2.s^{-1}$), ρ is fluid density ($kg.m^{-3}$) and c_p is the specific heat capacity ($J.kg^{-1}.K^{-1}$). V is the volume (m^3) and A is the surface area of the can (m^2). ($2V/A$) represents the characteristic dimension representing the specific geometry. In the case of the vertically placed cylindrical can, this characteristic dimension is equal to $H/(1+H/r)$. Here H is the height of the can (m) and r is the radius of the can (m). It was expected that equation (3) and equation (4) can be used to carry out data reduction to yield a single relationship for the dimensionless SHZ temperature and the Fourier number.

Using the CFD generated data sets for 7 different cases (see Table 1 and Figure 1) and the kind of normalisation as outlined above, 'Figure 5 of the original paper' was produced to show the uniqueness of this data reduction (reproduced here as Figure 2).

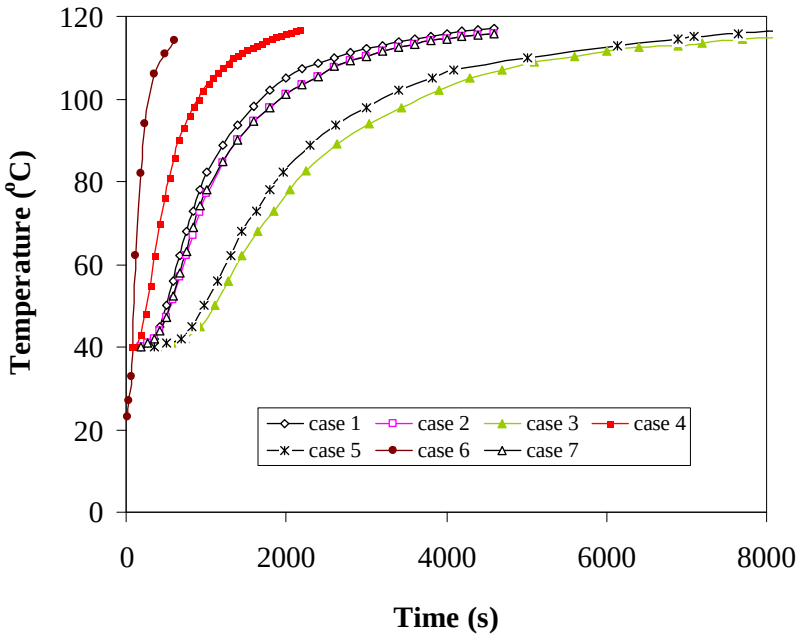

Figure 1. CFD simulated data as the 'experimental data sets' for establishing the correlation of θ^* versus F_o as defined in equations (3) and (4) (Cases referred to Table 1).

They found this was approximately the case for a wide range of viscosity and can sizes evaluated.

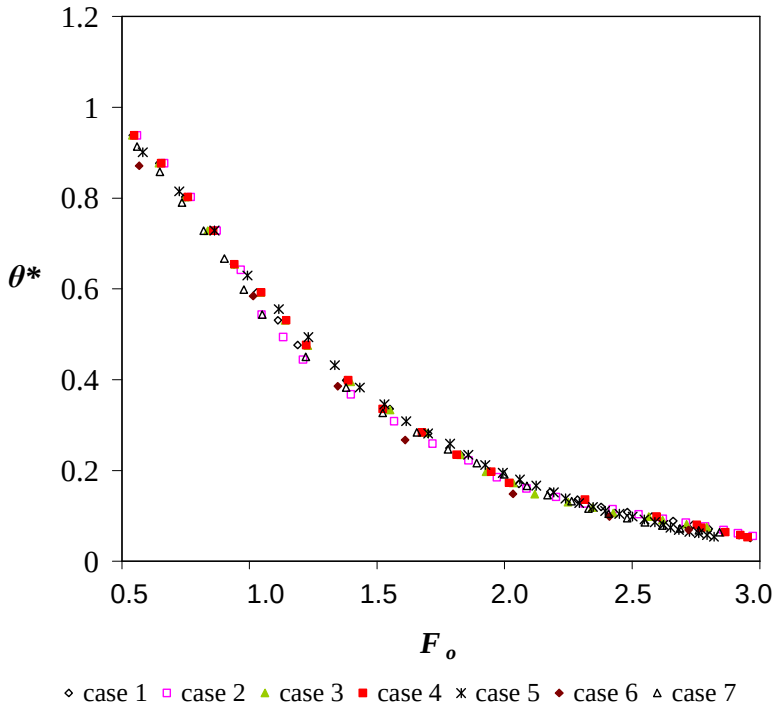

Figure 2. 'Generalised' correlation for the dimensionless SHZ temperature as a function of Fourier number.

Figure 2 was proposed to represent the capability of determining sterilisation time needed for any liquid food contained in a can of any size, within the range the tested. This range meant: the liquids with viscosity varying five orders of magnitude and a wide range of can sizes.

Table 1. Can geometries and types of liquids used in the seven CFD simulations carried out to generate the 'raw' data for data reduction using the effective thermal diffusivity approach

Case study	Can dimension (radius, height) (cm)	Position	Fluid used*
1	4.08, 11	Vertical	CMC
2	3.5, 15	Vertical	CMC
3	7, 30	Vertical	CMC
4	4.08, 11	Vertical	Fluid with a viscosity10 times of CMC
5	4.08, 11	Vertical	Fluid with a viscosity1/10 of CMC
6	4.08, 11	Vertical	Water
7	4.08, 11	Horizontal	Carrot-orange soup

**For CMC type fluids, thermal expansion coefficient is taken to be constant (0.0002 K^{-1}); carrot-orange soup (0.0002) also; The densities for CMC type solutions and the soup are taken to be 950 and 1026 $kg.m^{-3}$ respectively; specific heat capacities 4100, 3880 $J.kg^{-1}.K^{-1}$ respectively; thermal conductivities 0.7, 0.596 $W.m^{-1}.K^{-1}$.*

They arrived at, similar to that of the pure conduction problem, using the data generated for a number of combinations of can sizes, viscosities and densities with CFD and collapsing these data points with the definitions in equation (3) and (4), a simple relationship was deduced (the maximum SHZ temperature attained was about 115 °C):

$$\theta^* = 1.96e^{-1.2F_o}, \text{ for } F_o > 0.56$$
$$\theta^* = 1, \text{ for } F_o < 0.56 \quad (5)$$

The overall data spread of this unique relationship shown by these authors was at most $\Delta\theta^* \approx 0.087$ (or in real term $\Delta T \approx 7$ °C). At the critical value of F_o = 0.56, the error range is about 9%. Therefore, one may say that the process that involves a strong first order process (convection) is converted to a second order (conduction type) process with varying thermal 'conductivity'.

The exponent on the term (H/δ) in equation (2) was proposed to be positive 0.25, in order to match the data obtained by CFD for calculating the SHZ temperature. This was attributed to different geometry of concern (Farid and Ghani, 2004). This has a significant impact on predicted values as this gives sometimes up to 100% increase in Nusselt number thus affecting the scale of F_o. Furthermore, this implies that the heat transfer coefficient would increase with increasing height of the enclosure, which may be questionable. On the other hand, the sort of good agreement may be attributed to the generic nature of the property dependence of the Nusselt number as described in equation (2).

In the pure conduction problem, the SHZ is located at the centre of the geometry but here, the SHZ is a moving target. For pure conduction, the dimensionless temperature departs from the unity earlier for infinitely large Biot number (say at Fourier number of about 0.1 or 0.2 for the infinitely long cylinder geometry). For very large viscosity values ($\mu \to \infty$), the food would be solid like, thus little circulation within the can, hence little convection effect. In this extreme case of thermal sterilisation of food liquid, its θ^* - F_o relationship should be the quite similar to the pure solid case (the *Heisler* chart).

Re-working through the analysis, the current authors assessed the previous results and Figure 3 is the result of the analysis done by the current authors (note here for water, the thermal expansion coefficient was also taken as 0.0002 K^{-1} and in the current analysis, all thermal conductivity, specific heat capacity were taken as temperature dependent). It is arguable about which critical F_o should be chosen in equation (5) in order to minimise large error in this beginning state. 0.56 seems too large. The exponent for the term (H/δ) in equation (2) is also set at 0.25.

Note here that Case 6 is for water and a constant thermal expansion coefficient for water (i.e. 0.0002 K^{-1}) was used. This is the same as that taken for the CMC solutions (Cases 1-5). The thermal conductivity was taken to be the value corresponding to the average of 20 and 121°C, which is 0.67 $W.m^{-1}.K^{-1}$. The water behaviour appears to be slightly different from the other ones.

If one used 0.0004 K^{-1} as being the water thermal expansion value, this can cause large deviation from Figure 3. If we applied this 0.0004 K^{-1} to all the cases, however, the curves would gather together except that the F_o range has become larger (see Figure 4). As such, one may state that for constant thermal expansion coefficient, the CFD generated the temperature-time profiles for the SHZ zones of different fluids would be correlated using this approach.

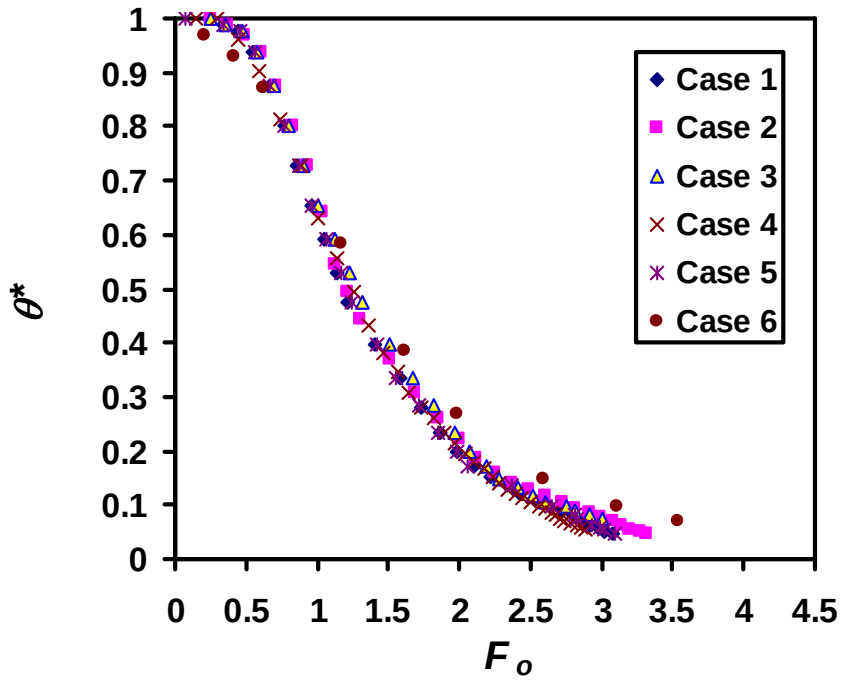

Figure 3. The corrected relationship obtained by re-working on the CFD data on various cases (Data from Farid and Ghani, 2004).

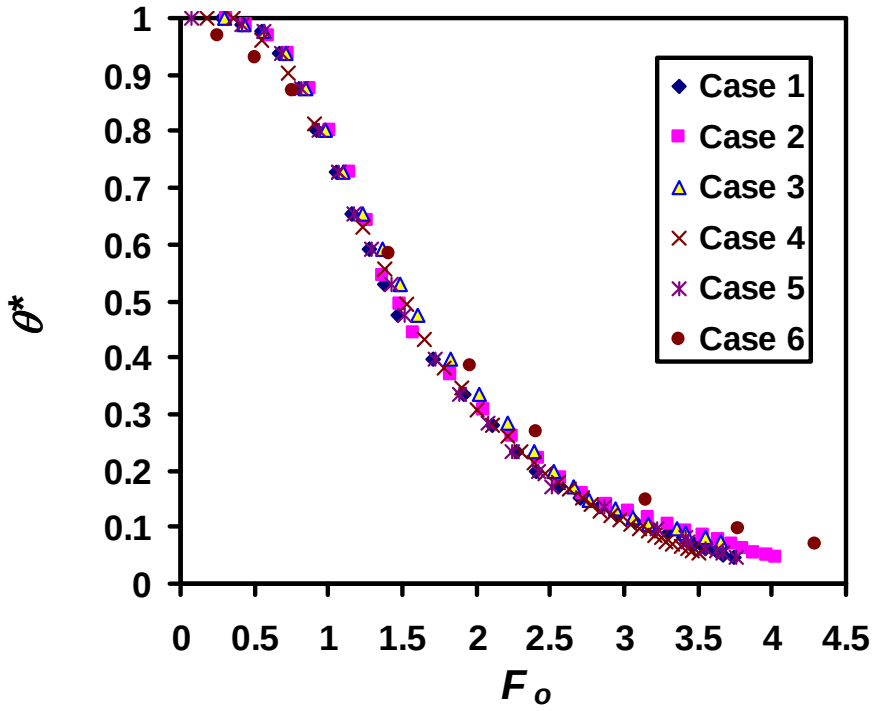

Figure 4. Relationship obtained when taking the thermal expansion coefficient all constant (0.0004 K^{-1}).

When we used temperature dependent thermal expansion coefficient for water (Table 2), the result is again different (see Figure 5). For water, this coefficient changes from 0.00021 at 20°C to 0.00075 at 100 °C. Here, we tested this also with the temperature dependent water density and specific heat capacity of water.

If one used this temperature dependent thermal expansion coefficient to replace the constant one (0.0002 K^{-1}) in all cases, again the corresponding curves will collapse together but in yet another different range of F_o (see Figure 6). This suggests that if CFD simulations were based on this variable thermal expansion coefficient (the same one as water for instance) for all the fluids, good correlation between θ^* and F_o would also be obtained.

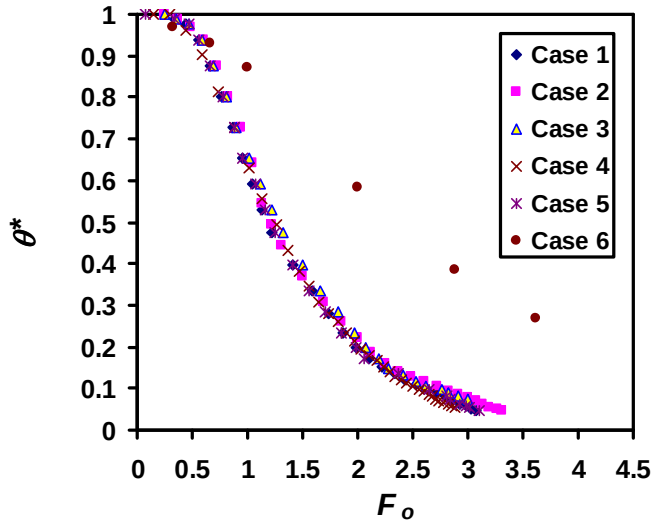

Figure 5. The same simulated results as in Figure 3, except for Case 6 (water), where the variable thermal expansion coefficient is used.

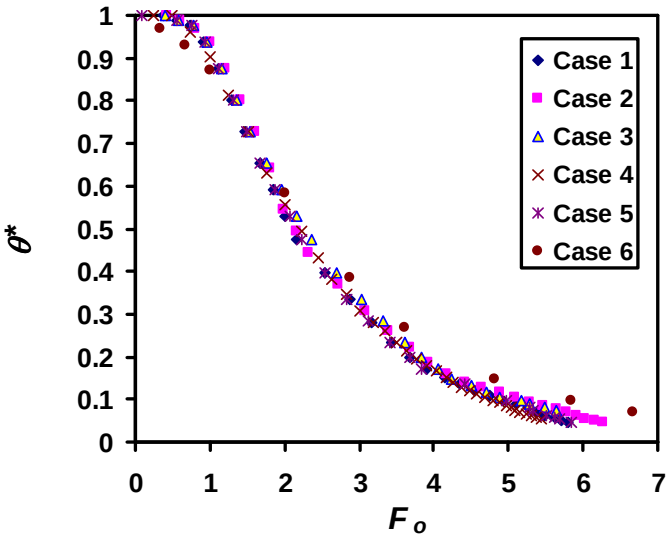

Figure 6. The calculation results for variable thermal expansion coefficient (using the water value for all the fluids).

At this point, it may be summarised that when the physical properties of the fluids are similar in trends (in their temperature dependence functions), there is a likelihood of a good correlation between θ^* and F_o. This is already a nice surprise, considering the SHZ temperature point (or location) moves with time.

One practical point can be made at this stage is about the suggestion of using an average Nusselt number, as made by the authors of the original approach to obtain F_o for use in equation (6) (which would be of different value from the that used in the CFD for generating the raw data, i.e. different from the 'experimental condition'), can cause appreciable errors. Figure 7 shows when using the average *N*u, Case 1 deviates from the original relationship shown in Figure 3.

Table 2. Relationships for Evaluating Water Properties

β = -4.160 x $10^{-8}T^2$ + 1.129 x $10^{-5}T$ - 8.148 x 10^{-6}, r^2 = 0.999
c_p = 0.011 T^2 - 0.963 T + 4199.245, r^2 = 0.988
ρ = -0.0033 T^2 - 0.0964 T + 1001.2, r^2 = 0.999
$k = 0.57109 + 0.0017625 \cdot T - 6.7036 \times 10^{-6} \cdot T^2$ (Rahman, 1995)
$\mu = 2.3378 \times 10^{-3} - 4.5168 \times 10^{-4} \ln T$, r^2 = 0.995

Following on from the above calculations to explore the 'generality' of the approach, we have gone back to the original *Heisler* chart approach to seek an answer to the question "is there a reason for such an approach to be causing errors?

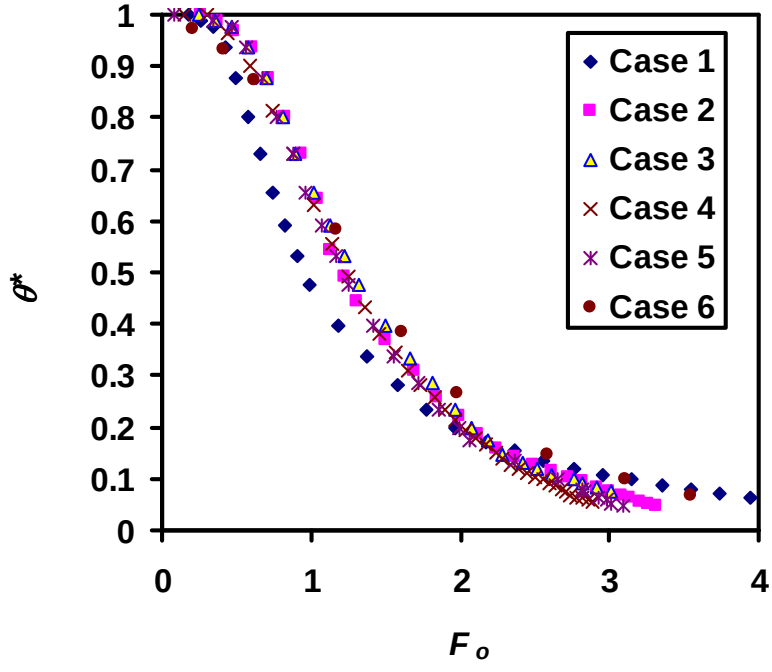

Figure 7. Case 1 deviates from the original plot in Figure 3, when the average *Nu* is used.

One can note that the CFD generated data sets or the case studies in Table 1 have the following commonalities: For CMC based fluids, though viscosity was varied, the thermal expansion coefficient, density and specific capacity were the same and they were

constant. When the viscosity was lowered by a factor of 10 or increased by 10 times, the viscosity changes with temperature in the same way (i.e. the viscosities were all proportional to μ_{CMC}). The carrot-orange soup's properties, apart from viscosity, were also made constant. Its viscosity influence on *Nu* calculation is almost the same as that for the CMC solution (Case 1). Water properties used were also constant except the viscosity.

Here we look at the *Heisler* chart approach or the similarity approach, it can be noted that the unique relationship was established for constant Biot number (*Bi*) (constant heat transfer coefficient *h* and constant thermal conductivity *k*). For example for one dimensional heat conduction, the partial differential equation is exactly the following:

$$\frac{\partial \theta^*}{\partial F_o} = \frac{\partial^2 \theta^*}{\partial x^{*2}} \tag{6}$$

where F_o is proportional to *t* with constant physical properties, i.e. $F_o = \alpha \cdot t / L^2$. Thermal diffusivity α is constant. The dimensionless distance x^* is *x*/*L*, where *L* is the half thickness of the slab (m). The dimensionless temperature θ^* is:

$$\theta^* = \frac{T_\infty - T\left(x^*, t\right)}{T_\infty - T_o} \tag{7}$$

Thus one expects that, for constant *Bi*,

$$\theta^* = f\left(x^*, F_o\right) \tag{8}$$

The results were generated by exact or numerical solutions for centre ($x^* = 0$) or average temperature. The lowest temperature (when heating) is located at the centre of the geometry and does not move as the SHZ location.

As such, for different (but constant properties like *k* and *h*), unique correlations exist. The 'constant' nature seems to be the critical issue for unique (reduced) relationship to be established. If the Fourier number in equation (8) is variable against temperature and the dependence function varies from material to material, equation (8) may not generate a unique relationship that applies to all materials.

$$\theta^* = f\left(x^*, \frac{\bar{k}_j}{\rho_j\left(\theta^*\right) c_{p\,j}\left(\theta^*\right)} \cdot \frac{t}{L_j^{\,2}} \right) \tag{9}$$

where *j* denotes material type. Here the thermal conductivity is taken to be an average value to simplify the situation. One can see, on the other hand, if the temperature dependence function for each property is similar among all materials, equation (9) may also produce the similar dimensionless temperature profile against dimensionless distance. There is no strict proof of this at this stage.

Relating this to the argument of the effective thermal diffusivity approach, we can see that for all CMC type fluids, data reduction can be achieved successfully (as shown in Figure 3).

Indeed, the CFD calculations reported in the effective thermal diffusivity approach (Farid and Ghani, 2004) involved properties of similar nature. Though the range of viscosities was large but their temperature dependencies were similar (see Figure 8). Figure 8 has been plotted this way because the *Ra* number is proportional to μ^{-1} and Nusselt number or Fourier number is proportional to $Ra^{0.28}$. The water one gives the largest possible deviation in the fluids tested (see Figure 3) due to its sharper rise in $\mu^{-0.28}$. The predicted film properties do not change drastically at all in the film temperature range, which is narrow in the original study (besides the case for water, which starts at 70.5 °C, the viscous fluids all start from 80.5 °C). It would have been interesting to see what the effect of initial temperature (say when it is much lower) is on the sterilisation process.

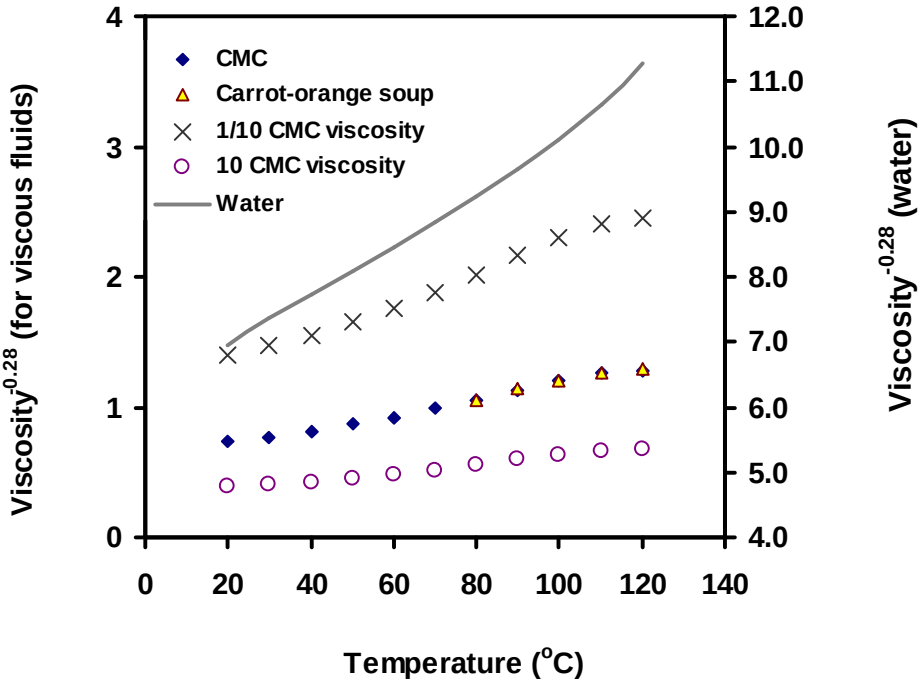

Figure 8. Effect of temperature on (viscosity)$^{-0.28}$ of the fluids investigated in Cases 1-7 (Table 1).

As such, one may conclude that when the physical properties are either constant or have the similar temperature dependence functions, there is a likelihood of the successful data reduction using the effective thermal diffusivity approach as outlined by Farid and Ghani (2004). This is a positive outcome, based on the limited cases investigated so far. However, this needs more rigorous proof. The fluids which are of practical interest to food industry may have different temperature dependence functions, especially those that have reactions like starch gelatinisation or protein aggregation,

forming highly viscous and gel like materials. Their properties would have to be tested for validity of this approach as well as for the second approach to be outlined shortly.

So far, we have analysed in a quantitative manner the effective thermal diffusivity approach to data reduction. It has been shown that a wider range of fluid behaviours needs to be evaluated before such an approach can be adopted for the safety in food preservation.

3. THE EFFECTIVE VELOCITY APPROACH

The idea of preserving the first order (convection) influence in the mathematical formulation of the sterilisation or thermal processing in general was originated in 2002. In analysing this approach, only the vertically placed cylindrical can (which is filled completely by a liquid) is considered to limit the scope of applicability at present.

Firstly, we re-visit the early studies of Ghani (2002) and Ghani et al (1999). It has been demonstrated that the main features of the fluid flow pattern and temperature distribution and their evolution during sterilization. One typical result using CMC as a sample viscous fluid is shown in Figure 9. There are two circulation regions can be identified (Figure 9 (a)): one is near the side of the cylindrical section and one is located at the central region of the bottom surface. The occurrences of these two regions result in the kind of temperature distribution shown in Figure 9 (b), which can be interpreted as shown in Figure 10. The slowest heating zone has been found to be very close to the bottom surface and a rather gradual temperature reduction from the top to the bottom of the can.

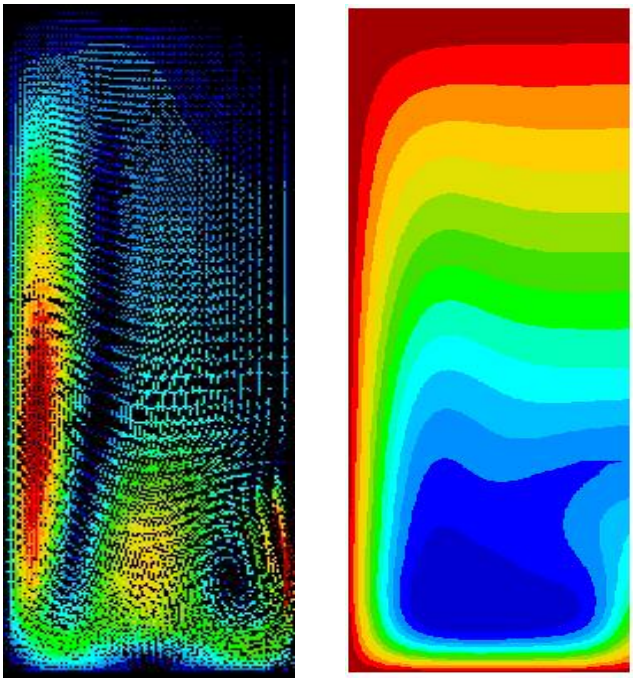

(a) (b)

Figure 9. Velocity contours of a can filled with CMC after being heated by steam condensation for 1157 seconds (the left side is the can side wall; the right side is the centre axis of the can) (kindly provided by Ghani, 2002).

Figure 10(a) shows an illustrative interpretation of the heating process. When only the bottom plate is heated and the other parts of the container are colder, the circulation starts from the fluid rising from the bottom plate surface. Figure 10(b) shows that if the bottom plate is colder and the wall of the cylindrical section is heated (the top may also be heated), then the circulation should start from the hot side wall surface and move up to the top due to buoyancy effect and then drop down to the lower region due to the gravity effect. As such, when all the sides are heated including the bottom plate, there are at least two recirculation regions when compete against each other forming the pattern that is shown in Figure 10(c). For different physical properties of the fluid of concern, and the variation in the height to diameter ratio, the ratio of the size of the side region circulation to that of the bottom region should vary.

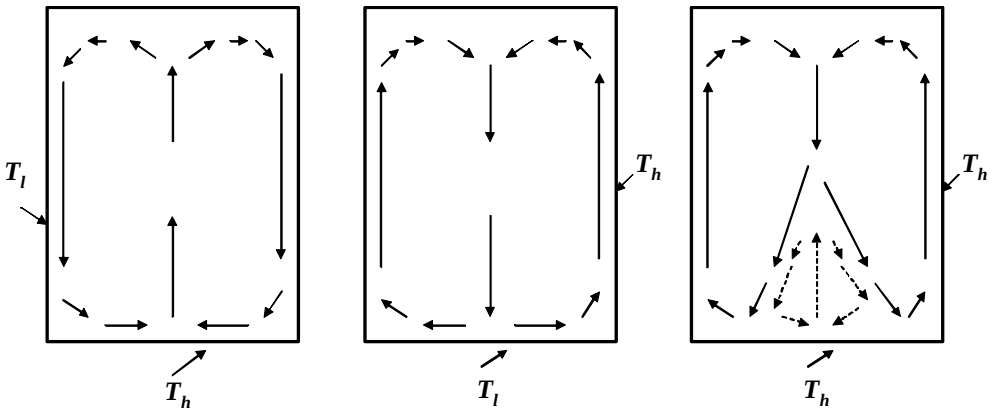

Figure 10. Physical interpretation of the flow field.

Further, one can interpret the interaction between the fluid flow current and the location of the SHZ as in Figure 9. It shows that the main fluid flow pathway corresponds the where about of the coldest zone.

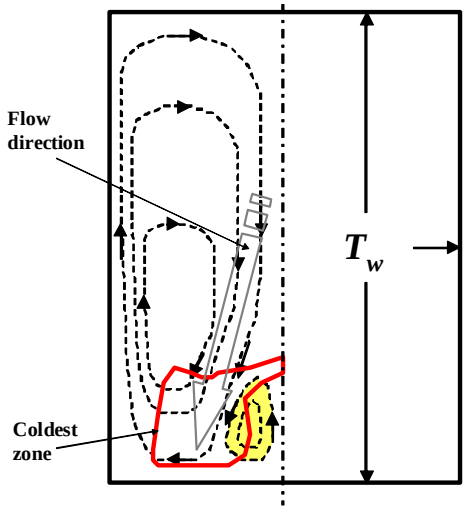

Figure 11. Illustration of the interaction between the flow field and the SHZ.

Figure 11 shows more explicitly such a phenomenon. As such, it is possible that the effect of natural convection may be grossly viewed in a one–dimensional manner, i.e. a one-dimensional heat transfer affected by an overall downward fluid (at a velocity generated due to natural convection effect).

Due to the above interpretation of the physics involved, a one-dimensional thermal processing equation may be written:

$$\rho \cdot c_p \cdot \frac{\partial T}{\partial t} = \frac{\partial}{\partial z}\left(k \frac{\partial T}{\partial z} \right) - u_z \cdot \rho \cdot c_p \cdot \frac{\partial T}{\partial z} \tag{10}$$

At $z = 0$ and $z = H$ (height of the container), $T = T_\infty = 121$ °C. At $t = 0$, $T = 20$ °C. One can see that the pathway of the downwards current is limited (approximately by nature) to the vertical height of the can. It is therefore expected in the early stage of this work that the very tall can (height is much larger than the diameter) would not be 'interpreted' well by this approach (despite this kind of can may not be that commonly used in practice). The physical properties are taken at the initial film temperature $T_{film} = (T_\infty + T_i)/2$ for simplicity, where T_i is the initial temperature.

Based on the analysis of Guo (1992), when the viscous force is in the same order of magnitude as the buoyancy force (this is more likely the case for can sterilisation), the velocity can be shown analytically by dimensional analysis of the Navier-Stokes equation for natural convection to be the following

$$u_z \propto \frac{\beta(T_{film}) \cdot g \cdot (T_\infty - T) \cdot \delta^2}{\mu_l(T_{film}) / \rho_l(T_{film})} \tag{11}$$

When the inertia force and buoyancy force is of the same order, this velocity should be written as:

$$u_z \propto \left[\beta(T_{film}) \cdot g \cdot (T_\infty - T) \cdot \delta \right]^{0.5} \tag{12}$$

It is likely, due to the complexity of the momentum transfer illustrated by the original Navier-Stokes equations, equation (10) is indeed a very simplified version. In any case, this equation would be a good start to look at the problem. This equation may not be correct for large height-to-diameter ratios, as the momentum gained by the accelerating fluid along sufficiently long heated wall can be great and the downward flow generated may not be described by equation (11) anymore. To this end, equation (12) may be more appropriate. Perhaps a kind of partition between the two equations would be a more appropriate method. This is beyond the scope of the current study.

Similarly, δ is the characteristic length of the can. For simplicity, it is also taken as the radius r_o (m). As mentioned above, the real situation in a can may be somewhere in between equation (7) and (8). To which end this process would swing may strongly depend on the viscosity.

Except the horizontal can for the Carrot-orange soup (Case 7) and the hall can (Case 3), the other cases have been analysed. The most important task is to see if equation (10) combined with equation (11) can adequately represent the detailed features

of the heating process, i.e. the temperature-time curves and the location of the SHZ relative to the can height. To start with, equation (11) can be made as follows:

$$u_z = \lambda \cdot \frac{\beta\left(T_{film}\right) \cdot g \cdot \left(T_\infty - T\right) \cdot \delta^2}{\mu_l\left(T_{film}\right) / \rho_l\left(T_{film}\right)} \tag{13}$$

The function λ (dimensionless) represents the geometrical influence (a shape factor, scaling according to H/r) and also the possible property influence (e.g. the viscosity or more probably the kinematic viscosity).

$$\rho\left(T_{film}\right) \cdot c_p\left(T_{film}\right) \cdot \frac{\partial T}{\partial t} = \frac{\partial}{\partial z}\left(k\left(T_{film}\right) \cdot \frac{\partial T}{\partial z} \right) - \lambda \cdot \frac{g \cdot \beta\left(T_{film}\right) \cdot \rho\left(T_{film}\right)^2 \cdot c_p\left(T_{film}\right) \cdot \delta^2}{\mu\left(T_{film}\right)} \cdot \frac{\partial T}{\partial z} \tag{14}$$

A *Matlab* program was established to perform various tasks to investigate this new approach. Essentially it solves equation (14) for the temperature-distance, velocity-distance profiles at different timings of a sterilisation process. Figure 12 shows the individually simulated SHZ temperature-time profiles for the vertically placed cans (Case 1, 2, 4, 5 and 6). For constant and individual λ value, equation (14) can be shown to do reasonably well. No deliberate attempt was made to try matching more exactly the profiles at this stage of exploration. Nevertheless conservative predictions (generally but only slightly lower temperature than the CFD solutions) have been obtained (see Figure 12). Table 3 summarises the fitted λ values.

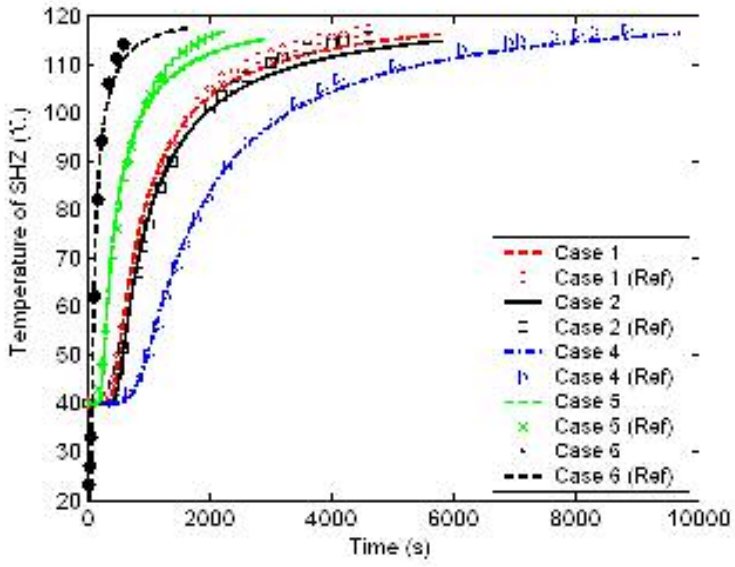

Figure 12. Comparison between the calculations made using equation (14) with the appropriate boundary conditions and that of the CFD generated 'experimental' data.

Figure 13 shows the temperature-distance (Z is z/H; Can top: Z = 0) profiles at different timings of the process. The SHZ tends to stay in the region between 5 to 20% of the height from the bottom of the can. This matches well with the CFD simulations, though CFD simulations can also tell where this SHZ is as far as the radial direction is concerned.

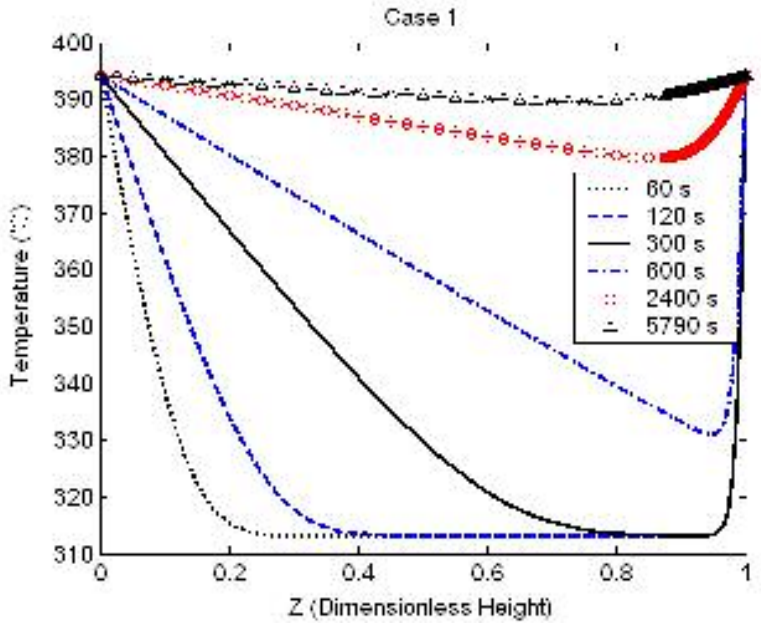

Figure 13. The evolution of the heating profile for Case 1 as predicted using equation (14).

Table 3. Fitted λ values

Case study	Can dimension (radius, height) (cm)	λ	Fluid used
1	4.08, 11	6.8103×10^{-4}	CMC
2	3.5, 15	1.1792×10^{-3}	CMC
3	7, 30	–	CMC
4	4.08, 11	3.1104×10^{-3}	Fluid with a viscosity10 times of CMC
5	4.08, 11	1.3878×10^{-4}	Fluid with a viscosity1/10 of CMC
6	4.08, 11	7.5102×10^{-7}	Water
7	4.08, 11	–	Carrot-orange soup

Figure 14 shows the heating profile generated for the fluid that has 10 times greater viscosity than the original CMC solution (Case 4). One can see that the development of the SHZ is not as sharp as that shown for Case 1. The process is more gradual. When the viscosity is lowered, as in Case 5 and in Case 6 (water) the SHZ becomes a more of a 'kink' as heating progresses (results not shown here). It has been revealed that the predicted SHZ initially gets narrowed and pushed downwards, but then moves up towards the final temperature stage. This is an interesting insight as towards the

end of the heating the driving force for natural convection is sharply reduced. The conduction effect may become more important to 'drive' the SHZ towards the centre (kind of 'going back' to the behaviour of a solid medium). This appears to happen more so in the highly viscous fluid.

Figure 15 shows the corresponding u_z locations in Case 1 (see Figure 13 also). This is essentially a mirror image of the temperature-distance profiles, as the velocity is proportional to the temperature diference.

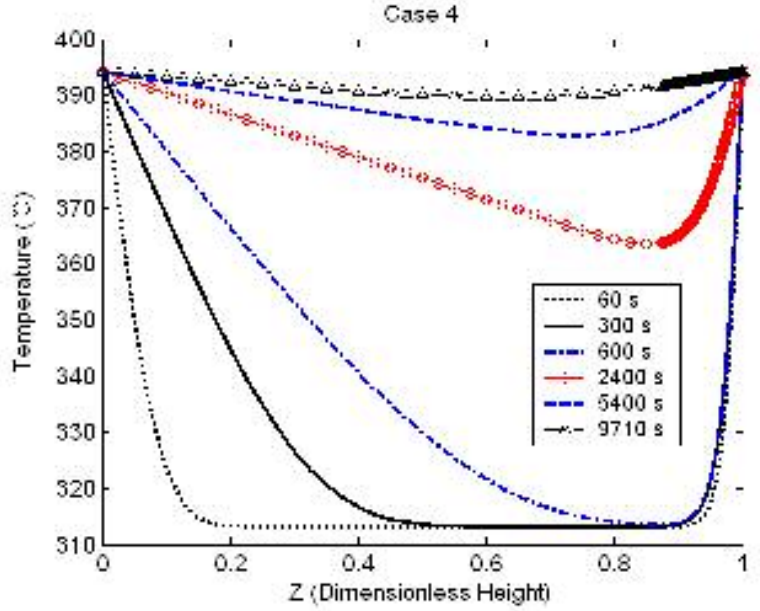

Figure 14. The prediction using equation (14) for Case 4.

Figure 16 shows the maximum velocity changes with time for Case 1. It characteristically changes from a high value (due to the initially large temperature driving force) towards very low value (due to the diminishing temperature difference at the end of the sterilisation process). Figure 17 shows this maximum velocity reduction over time for the case when water is used. Its initial value is higher than that of the CMC solution which is expected due to the low viscosity. One can see that this reduction has occurred also more rapidly than that of CMC solution (Case 1) as water is more fluidic than the CMC solution thus achieving the desired temperature level much more quickly. The range of the velocities obtained from fitting the model can be seen to be in the same order of magnitudes as those predicted using CFD (Ghani, 2002). As mentioned earlier that the function λ is expected to be affected by the kinematic viscosity, for the same geometrical dimensions (Case 1,4,5,6), one can establish an emipirical relationship to show the general trend. According to Figure 18, we have the following:

$$\lambda \approx 0.108 \cdot \gamma^{0.725} \qquad (15)$$

The coefficient 0.108 would change if another set of geometrical data is considered. With the above equation, we can further write (for this fixed geometry as in Case 1), the following velocity equation is expected:

DOI: 10.2202/1556-3758.1006

$$u_z \approx 0.108 \frac{\beta\left(T_{film}\right) \cdot g \cdot \left(T_\infty - T\right) \cdot \delta^2}{\gamma_{film}^{0.275}} \tag{16}$$

This indicates that the viscosity dependence is weakened because of the inertia forces which play a role too in such a process.

Overall, one can observe that the effective velocity approach has captured the key features of the natural convection driven thermal processing. Mathematically, this is done by combining the first and second order processes which are known to occur in such situations.

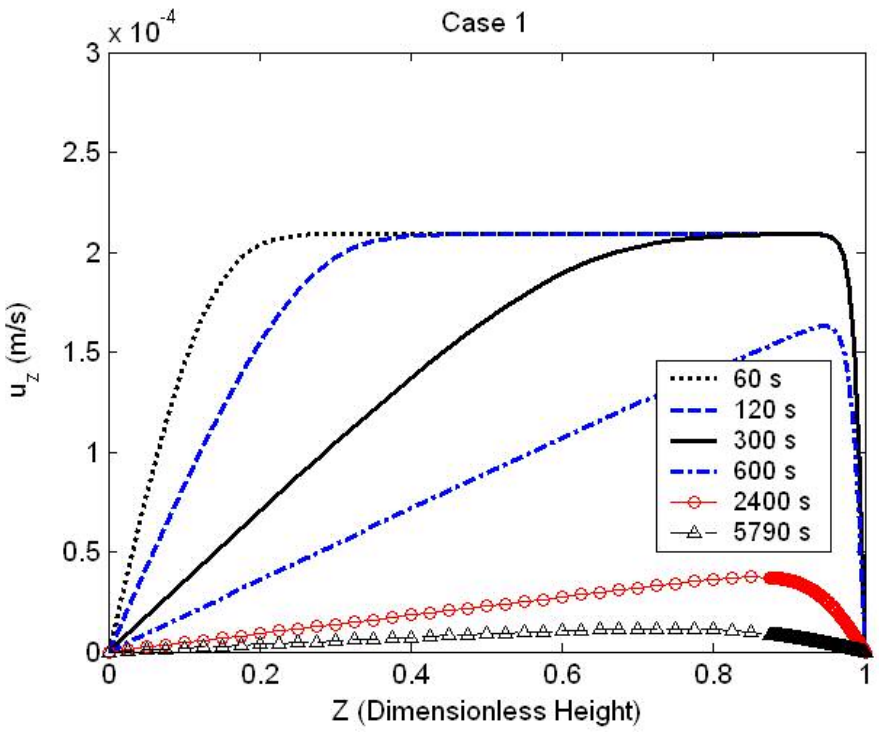

Figure 15. Velocity distribution in Case 1 at different timings.

4. CONCLUSIONS

In this study, careful analysis has been conducted to investigate two approaches to developing simple correlations for thermal processing. The recent effective thermal diffusivity model has been benchmarked and the advantages of the approach shown. The sensitivity (or the uniqueness) of the model approach against the temperature dependent physical properties has been highlighted. The second approach, which is new and may be called the 'effective velocity approach' has been illustrated. It has been demonstrated that by preserving the first order effect (i.e. the convection effect) in the heating equation, the effective velocity approach provides an opportunity to correlate with good accuracy the experimental data (generated by the CFD). In the second approach, the essential features of the natural convection driven process can be seen to be captured well. The predicted circulation velocity level matches well with the previous CFD simulations for the two

dimensional situations. Despite the apparent success so far in using the simple models, the sensitivity of these simple models to variations of physical properties is a major concern when come to applying these approaches in practice. In order to generate more reliable CFD data sets for benchmarking the simple model approaches, more realistic and accurate physical properties must be used. In particular, the temperature dependencies of these physical properties (like thermal expansion and viscosity) need to be quantified more accurately. Finally, there is a possibility to obtain a conservative bound solution to this problem instead of trying to obtain the exact values. This may ensure the practical safety if such predictions are used. In any case, it is not safe to use these simple approaches in practice just yet.

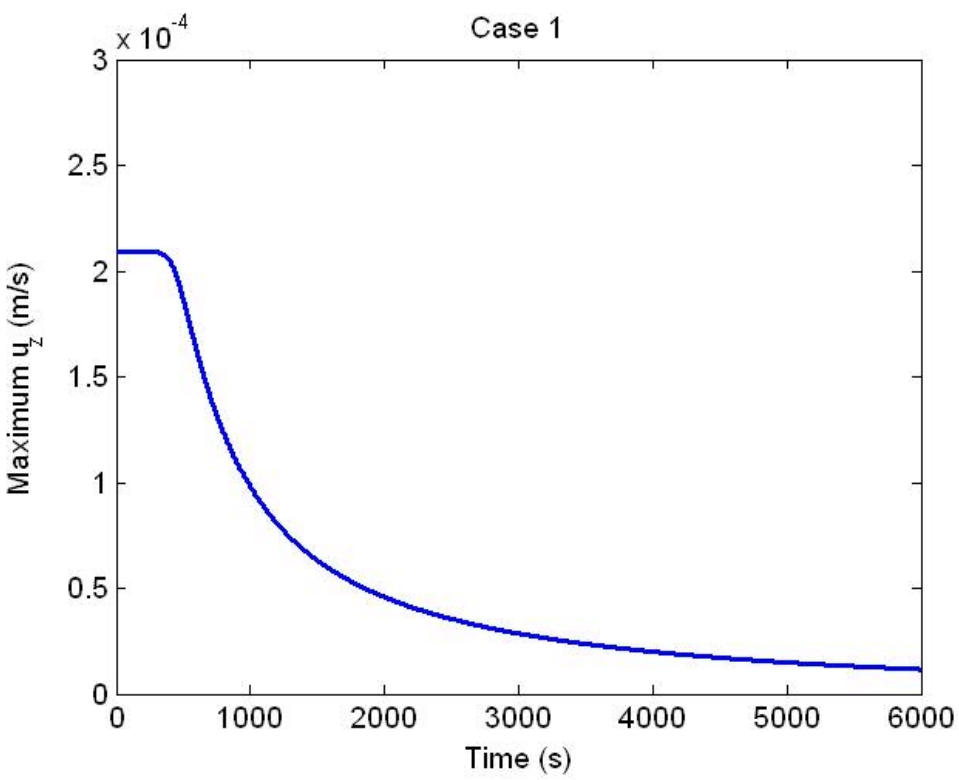

Figure 16. Change in the maximum velocity against time of sterilisation in Case 1.

DOI: 10.2202/1556-3758.1006

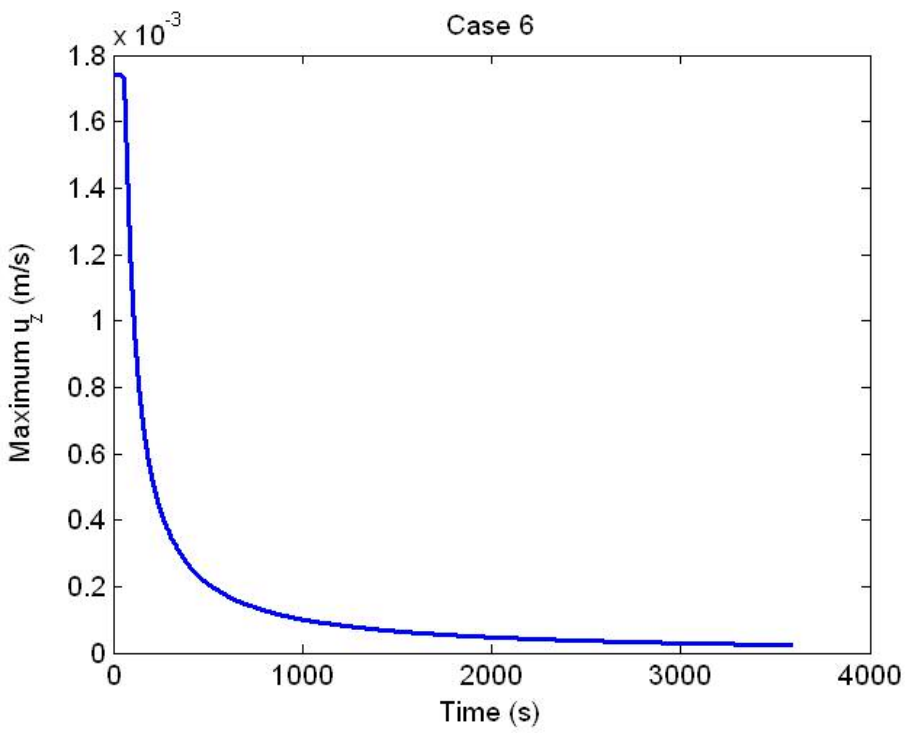

Figure 17. Change in the maximum velocity against time of sterilisation in Case 6.

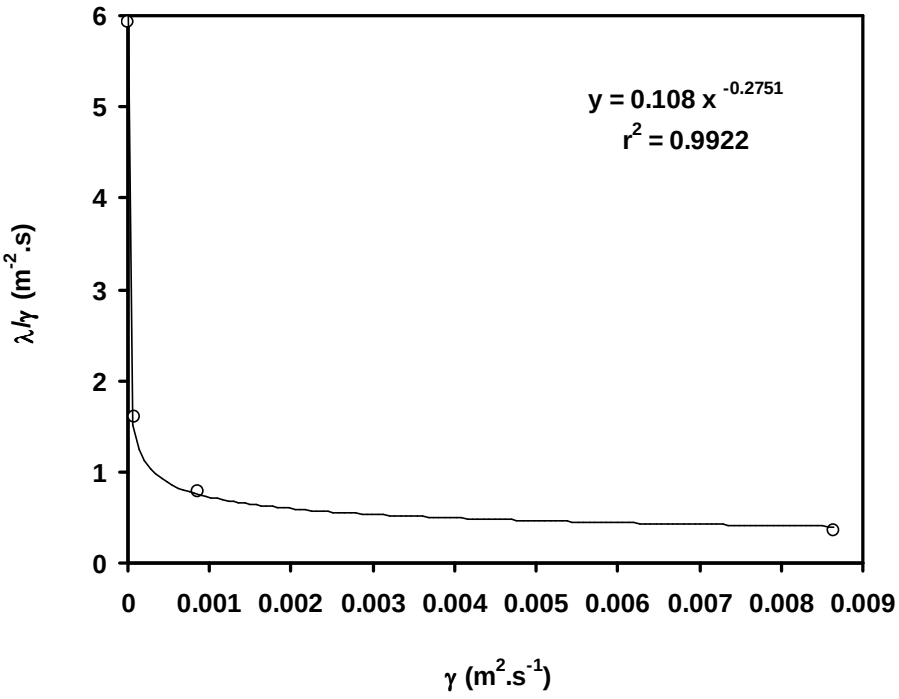

Figure 18. The function of the ratio of λ/γ against γ.

5. NOMENLCLATURE

δ characteristic dimension (m)
ρ density (kg.m^{-3})
γ kinematic viscosity (m^2.s^{-1}) (= μ/ρ)
α thermal diffusivity (m^2.s^{-1})
β thermal expansion coefficient (K^{-1})
θ* dimensionless temperature (defined in equation (3) or (6))
Bi Biot number
c_p specific heat capacity (J.kg^{-1}.K^{-1})
F_o Fourier number (defined in equation (4))
g gravity acceleration (m.s^{-2})
h heat transfer coefficient (W.m^{-2}.K^{-1})
H height of the can (m)
k thermal conductivity (W.m^{-1}.K^{-1})
Nu_δ Nusselt number $Nu = \frac{h \cdot \delta}{k}$
Pr Prandtl number ($= \frac{c_p \cdot \mu}{k}$)
r radius or radial coordinate (m)
Ra_δ Rayleigh number $Ra_\delta = \frac{g \cdot \beta \cdot \Delta T \cdot \delta^3}{\gamma}$
T temperature (°C)
t time (s)
T_∞ sterilisation temperature or steam condensing temperature (°C)
T_o initial temperature (°C)
T_{SHZ} temperature of the slowest heating zone (SHZ) (°C)
u velocity at *z* direction (m.s^{-1})
Z dimensionless distance along *z* (=*z*/*H*)
z vertical distance or coordinate (m)

ACKNOWLEDGEMENT

The authors would like to thank Dr. Abdul Ghani of the University of Auckland, for his kindness in providing the original CFD simulated data for us to work on.

REFERENCES

Datta, A.K., Teixeira, A.A. (1987) Numerical modeling of natural convection heating in canned liquid foods. Transactions of American Society of Agricultural Engineers, 30(5): 1542-1551

Datta, A.K., Teixeira, A.A. (1988) Numerically predicted transient temperature and velocity profiles during natural convection heating of canned liquid foods. Journal of Food Science, 53(1): 191-195

DOI: 10.2202/1556-3758.1006

Farid, M.M. and Ghani, A.G. (2004) A new computational technique for the estimation of sterilisation time in canned food. Chemical Engineering and Processing, 43, 523-531

Ghani, A.G. (2002) Thermal Sterilization of Canned Liquid Foods. PhD thesis, Department of Chemical and Materials Engineering, The University of Auckland, New Zealand.

Ghani, A.G., Farid, M.M., Chen, X.D. (2001) Thermal sterilization of canned food in a 3-D pouch using computational fluid dynamics. Journal of Food Engineering, 48, 147-156

Ghani, A.G., Farid, M.M., Chen, X.D. (2002) Numerical simulation of transient temperature and velocity profiles in a horizontal can during sterilization using computational fluid dynamics, Journal of Food Engineering, 51: 77-83

Ghani, A.G., Farid, M.M., Chen, X.D. (2002) Theoretical and experimental investigation of the thermal destruction of Vitamin C in food pouches. Journal of Computers and Electronics in Agriculture - special issue on "Applications of CFD in the Agri-food Industry", 34: 129-143

Ghani, A.G., Farid, M.M., Chen, X.D. (2002) Theoretical and experimental investigation on the thermal inactivation of *Bacillus stearothermophilus* during thermal sterilization in food pouches. Journal of Food Engineering, 51: 221-228

Ghani, A.G., Farid, M.M., Chen, X.D. (2003) A computational and experimental study of heating and cooling cycles during thermal sterilization of liquid foods in pouches using CFD. Journal of Process Mechanical Engineering, 217: 1-9

Ghani, A.G., Farid, M.M., Chen, X.D., Richards, P. (1999) An investigation of deactivation bacteria in canned liquid food during sterilization using computational fluid dynamics (CFD). Journal of Food Engineering, 42(4): 207-214

Ghani, A.G., Farid, M.M., Chen, X.D., Richards, P. (1999) Numerical simulation of natural convection heating of canned food by computational fluid dynamics. Journal of Food Engineering, 41(1): 55-64

Guo, Z.Y. (1987) Thermal Fluid Engineering, Tsinghua University Press, Beijing.
Holman, J.P. (1976) Heat Transfer, 4th Edition, McGRaw-Hill Kogakusha Ltd, Tokyo. pp.254-257

Kumar, A., Bhattacharya, M., Blaylock, J. (1990) Numerical simulation of natural convection heating of canned thick viscous liquid food products. Journal of Food Science, 55(5): 1403-1411

Rahman, M.S. (1995) Food Properties Handbook, CRC Press, N.Y.

Singh, R.P. and Heldman, D.R. (1993) Introduction to Food Engineering. 2nd Edition, San Diego: Academic Press.